Penerbit Akademia Baru

Journal of Advanced Research in Fluid Mechanics and Thermal Sciences

Journal homepage: www.akademiabaru.com/arfmts.html
ISSN: 2289-7879

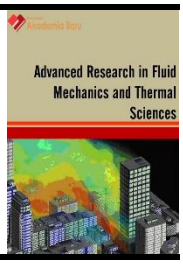

Effect of Hall Currents on Convective Heat and Mass Transfer Flow of a Viscous Electrically Conducting Fluid in A Nonuniformly Heated Vertical Channel with Radiation

Open Access

Madduleti Nagasasikala[1], Bommanna Lavanya[2,*]

[1] Department of Mathematics, Govt. Degree College (Autonomous), Anantapuramu-515001, A.P, India
[2] Department of Mathematics Assistant Professor Senior Grade MIT MAHE, Manipal-576104, KA, India

ARTICLE INFO

Article history:
Received 2 April 2020
Received in revised form 25 August 2020
Accepted 6 September 2020
Available online 14 October 2020

Keywords:
Convective; Hall Current Radiation; Heat and Mass Transfer

ABSTRACT

In the present document we inspect the deportation study of heat and mass transfer flow of a viscous electrically conducting fluid in a vertical wavy channel under the influence of an inclined magnetic fluid with heat generating sources. The walls of the channels are perpetuated at constant temperature and concentration. The equations reign over the flow heat and concentration are solved by employing perturbation technique with a slope δ of the wavy wall. The velocity, temperature and concentration distributions are investigated for a different value of Grashof number Hartmann number, Buoyancy ratio etc. The rate of heat and mass transfer are numerically estimated for a different variation of the governing parameters. It is found that higher the Lorentz force lesser the axial velocity in the flow region. An increase in the Hall parameter (m) enhances the axial velocity.

1. Introduction

The use of magnetic field of high intensity to an ionic liquid having less density, the conduction normal to the magnetic field is converted to curling of atomic particles and ions related to magnetic lines of force before occurring the clashing and a current induced perpendicular to both the electric and magnetic fields, is known as Hall effect. This effect is considered with heat or mass transfer analysis under the situation where the effect of the electromagnetic force is strong. Hall current is most prominent on the absolute value and orientation of the current density and thereby on the magnetic force term. Under the effects of Hall currents the convective flow problem with magnetic field is significant in view of engineering uses in electric transformers, transmission lines, refrigeration coils, power generators, MHD accelerators, nanotechnological processing, nuclear energy systems exploiting fluid metals, blood flow control and heating elements. In case of magnetic field of high

* *Corresponding author.*
E-mail address: lavanya.b@manipal.edu

https://doi.org/10.37934/arfmts.76.2.2642

strength and less density of the gas, the investigation of Magnetohydrodynamic flows with Hall current have the best utilizations in the study of Hall accelerators and flight Magnetohydrodynamic. Peristaltic flows have vast applications under the effects of applied magnetic field in the Magnetohydrodynamic feature of blood, process of dialysis, oxygenation and hypothermia. Exploration of non-Newtonian fluid flows has been the focus of many scientists due to its vast applications in industries and engineering. Important applications are existing in food engineering, petroleum production, power engineering, in polymer solutions and in melt in the plastic processing industries.

Many engineering and geophysical applications such as thermal insulation, geothermal reservoirs, cooling of nuclear reactors have hydro magnetic boundary layers connected with heat and mass transfer over a flat surface. Cooling of a molten liquid that is being stretched into a cooling system is used in many of the chemical engineering processes like metallurgical and polymer extrusion. Cooling liquid that is used and the rate of stretching has effect on the fluid mechanical properties of the last but one product. Some polymer fluids like Polyethylene oxide and Poly-isobutylene solution in cetane, that has better electromagnetic properties are normally used as cooling liquid because of the only reason that their flow can be adjusted by external magnetic fields for the improvement of the quality of the final product.

The flow of heat and mass from a wall embedded in a porous media is a subject of great interest in the research activity due to its practical applications, the geothermal processes, the petroleum industry, the spreading of pollutants, cavity wall insulations systems, flat-plate solar collectors, flat-plate condensers in refrigerators, grain storage containers and nuclear waste management. Coupled heat and mass transfer by natural convection in a fluid-saturated porous medium has attracted considerable attention in recent years due to many important engineering and geophysical applications such as cooling of nuclear fuel in shipping flasks and water filled storage bags, insulation of high temperature gas-cooled reactor vessels, drums containing heat generating chemicals in the earth, thermal energy storage tanks, regeneration heat exchanges containing catalytic reaction.

Coupled heat and mass transfer by natural convection in a fluid-saturated porous medium has attracted considerable attention in recent years due to many important engineering and geophysical applications such as cooling of nuclear fuel in shipping flasks and water filled storage bags, insulation of high temperature gas-cooled reactor vessels, drums containing heat generating chemicals in the earth, thermal energy storage tanks, regeneration heat exchanges containing catalytic reaction.

In recent years, energy and material saving considerations have prompted an expansion of the efforts at producing efficient heat exchanger equipment through augmentation of heat transfer. Radiative heat and mass transfer play an important role in manufacturing industries for the design of fins, steel rolling, nuclear power plants, and gas turbines. Various propulsion devices for aircraft, missiles, satellites and space vehicles are examples of such engineering applications. If the temperature of the surrounding fluid is rather high, radiation effects play an important role and this situation exists in space technology. In such cases, one has to take into account the effect of thermal radiation and mass diffusion. England and Emery [4] studied thermal radiation effects of an optically thin gray gas bounded by a stationary vertical plate. Radiation effects on mixed convection along an isothermal vertical plate were studied by Hossain and Takhar [5]. Raptis and Perdikis [6] studied the effects of thermal radiation and free convection flow past a moving vertical plate, the governing equations were solved analytically. Das *et al.,* [7] analysed radiation effects on flow past an impulsively started infinite isothermal vertical plate. Lavanya [8] studied effects of dissipation and radiation on heat transfer flow of a convective rotating cuo-water nano-fluid in a vertical channel. Nagasasikala *et al.,* [9] studied Effects of dissipation and radiation on heat transfer flow of a convective rotating cuo-water nano-fluid in a vertical channel. Nagasasikala *et al.,* [10] heat and mass

transfer of A MHD Flow of a nanofluid through a porous medium in an annular, circular region with outer cylinder maintained at constant heat flux.

The current development of magneto hydrodynamics application is toward a strong magnetic field (so that the influence of electromagnetic force is noticeable) and toward a low density of the gas (such as in space flight and in nuclear fusion research). Under this condition, the Hall current becomes important. The rotating flow of an electrically conducting fluid in the presence of a magnetic field is encountered in geophysical, cosmical fluid dynamics, medicine and biology. Application in biomedical engineering includes cardiac MRI, ECG, etc. Several engineering applications in areas of Hall accelerator as well as in flight MHD have been studied by the researchers. Ahmed and Kalita [11] studied transient MHD free convection from an infinite vertical porous plate in a rotating system with mass transfer and Hall current. Hayat *et al.,* [12] studied rotating flow of a third-grade fluid in a porous space with Hall current. Narayana *et al.,* [13] studied Hall current effects on free-convection MHD flow fast a porous plate. Rani and Tomar [14] studied thermal convection problem of micro-polar fluid subjected to hall current. Recently, Bakr [15] presented an analysis of MHD free convection and mass transfer adjacent to moving vertical plate for micropolar fluid in a rotating frame of reference in the presence of heat generation/absorption and a chemical reaction. Later, the same work was extended by Das [16] with thermal radiation effects. Lavanya and Nagasasikala [17] studied effects of chemical reaction and heat generation on the unsteady free convection flow past an infinite vertical permeable moving plate with variable temperature.

In the present paper we investigate the convective study heat and mass transfer flow of a viscous electrically conducting fluid in a vertical wavy channel under the influence of an inclined magnetic fluid with heat generating sources. The walls of the channels are maintained at constant temperature and concentration. The equations governing the flow heat and concentration are solved by employing perturbation technique with a slope δ of the wavy wall. The velocity, temperature and concentration distributions are investigated for a different value of G, M, m, Sc, N, N_1, α and x. The rate of heat and mass transfer are numerically evaluated for a different variation of the governing parameters. It is found that higher the Lorentz force lesser the axial velocity in the flow region. An increase in the Hall parameter (m) enhances the axial velocity. An increase in the strength of the heat generating source (α) leads to a depreciation in the axial velocity. It is found that higher the constriction of the channel walls larger |v| in the flow region. When the molecular Buoyancy force dominates over the thermal Buoyancy force.

2. Formulation of The Problem

We consider the steady flow of an incompressible, viscous ,electrically conducting fluid confined in a vertical channel bounded by two wavy walls under the influence of an inclined magnetic field of intensity Ho lying in the plane (y-z).The magnetic field is inclined at an angle α to the axial direction x and hence its components are $(0, H_0 Sin(\alpha), H_0 Cos(\alpha))$.In view of the waviness of the wall the velocity field has components(u,0,w)The magnetic field in the presence of fluid flow induces the current($(J_x, 0, J_z)$.We choose a rectangular Cartesian co-ordinate system O(x, y, z) with z-axis in the vertical direction and the walls at $x = \pm f(\frac{\delta z}{L})$ represented in Figure 1.

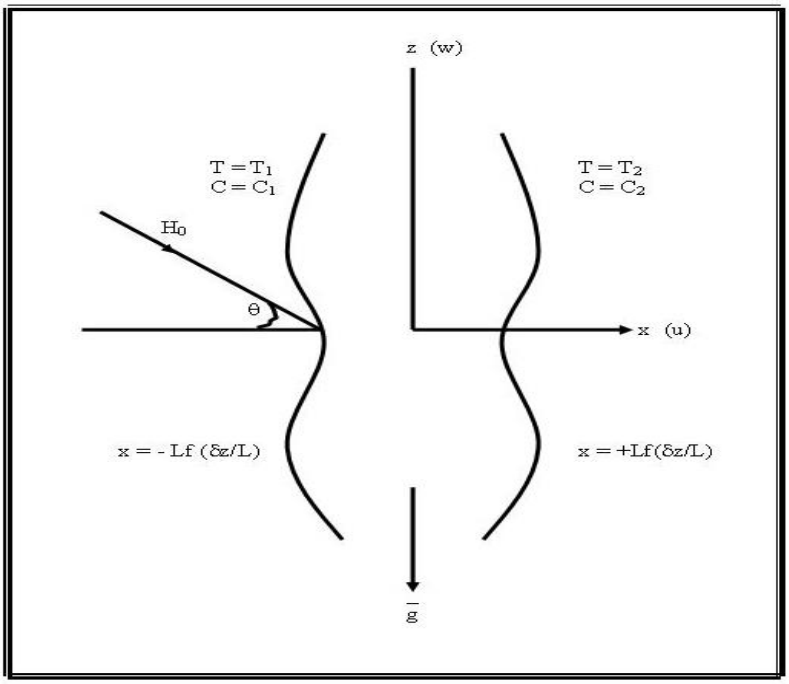

Fig. 1. Schematic diagram of the configuration

The equations governing the flow, heat and mass transfer in terms of the stokes stream function ψ are

$$\nabla^4\psi - M_1^2\nabla^2\psi + \frac{G}{R}\left(\frac{\partial\theta}{\partial x} + N\frac{\partial C}{\partial x}\right) = R\left(\frac{\partial\psi}{\partial z}\frac{\partial(\nabla^2\psi)}{\partial x} - \frac{\partial\psi}{\partial x}\frac{\partial(\nabla^2\psi)}{\partial z}\right) \quad (1)$$

$$Pr\left(\frac{\partial\psi}{\partial x}\frac{\partial\theta}{\partial z} - \frac{\partial\psi}{\partial z}\frac{\partial\theta}{\partial x}\right) = \nabla^2\theta - \alpha\theta + \frac{4}{3N_1}\frac{\partial^2\theta}{\partial x^2} \quad (2)$$

$$ScR\left(\frac{\partial\psi}{\partial x}\frac{\partial C}{\partial z} - \frac{\partial\psi}{\partial z}\frac{\partial C}{\partial x}\right) = \nabla^2 C \quad (3)$$

The boundary conditions are

$$\psi(f) - \psi(-f) = 1$$

$$\frac{\partial\psi}{\partial z} = 0, \frac{\partial\psi}{\partial x} = 0, \theta = 1, C = 1 \quad at \quad x = -f(\delta z)$$

$$\frac{\partial\psi}{\partial z} = 0, \frac{\partial\psi}{\partial x} = 0, \theta = 0, C = 0 \quad at \quad x = +f(\delta z)$$

3. Method of Solution

Introduce the transformation such that

$$\bar{x} = \delta x, \frac{\partial}{\partial x} = \delta\frac{\partial}{\partial\bar{x}}$$

Then,

$$\frac{\partial}{\partial x} \approx O(\delta) \rightarrow \frac{\partial}{\partial \bar{x}} \approx O(1)$$

For small values of δ <<1, the flow develops slowly with axial gradient of order δ and hence we take $\frac{\partial}{\partial \bar{x}} \approx O(1)$. Using the above transformation the Eq. (1)-(3) reduce to

$$F^4\psi - M_1^2F^2\psi + \frac{G}{R}\left(\frac{\partial\theta}{\partial x} + N\frac{\partial C}{\partial x}\right) = \delta R\left(\frac{\partial\psi}{\partial\bar{z}}\frac{\partial(F^2\psi)}{\partial x} - \frac{\partial\psi}{\partial x}\frac{\partial(F^2\psi)}{\partial\bar{z}}\right) \tag{4}$$

$$\delta P_1 R\left(\frac{\partial\psi}{\partial x}\frac{\partial\theta}{\partial z} - \frac{\partial\psi}{\partial z}\frac{\partial\theta}{\partial x}\right) = F^2\theta - \alpha_1\theta \tag{5}$$

$$\delta ScR\left(\frac{\partial\psi}{\partial x}\frac{\partial c}{\partial z} - \frac{\partial\psi}{\partial z}\frac{\partial C}{\partial x}\right) = F^2C \tag{6}$$

where

$$F^2 = \frac{\partial}{\partial x^2} + \delta^2\frac{\partial}{\partial\bar{z}^2}, \quad P_1 = \frac{3N_1P}{3N_1+4}, \alpha_1 = \frac{3N_1\alpha}{3N_1+4}$$

Assuming the slope δ of the wavy boundary to be small we take

$$\left.\begin{aligned}\psi(x,z) &= \psi_0(x,y) + \delta\psi_1(x,z) + \delta^2\psi_2(x,z) + \ldots\ldots\ldots\ldots\ldots\\ \theta(x,z) &= \theta_o(x,z) + \delta\theta_1(x,z) + \delta^2\theta_2(x,z) + \ldots\ldots\ldots\ldots\ldots\\ C(x,z) &= C_o(x,z) + \delta c_1(x,z) + \delta^2 c_2(x,z) + \ldots\ldots\ldots\ldots\ldots\end{aligned}\right\} \tag{7}$$

Let $\eta = \frac{x}{f(\bar{z})}$ (8)

Substituting Eq. (7) in Eq. (4)-(6) and using Eq. (7) and equating the like powers of δ the equations and the respective boundary conditions to the zeroth order are

$$\frac{\partial^2\theta_0}{\partial\eta^2} - (\alpha_1 f^2)\theta_0 = 0 \tag{9}$$

$$\frac{\partial^2 C_0}{\partial\eta^2} = 0 \tag{10}$$

$$\frac{\partial^4\psi_0}{\partial\eta^4} - (M_1^2f^2)\frac{\partial^2\psi_0}{\partial\eta^2} = -\frac{Gf^3}{R}\left(\frac{\partial\theta_0}{\partial\eta} + N\frac{\partial C_0}{\partial\eta}\right) \tag{11}$$

with

$$\left.\begin{aligned}\psi_0(+1) - \psi_0(-1) &= 1\\ \frac{\partial\psi_0}{\partial\eta} = 0, \frac{\partial\psi_0}{\partial\bar{z}} = 0,\ \theta_0 &= 1, C_0 = 1 \quad at \quad \eta = -1\\ \frac{\partial\psi_0}{\partial\eta} = 0, \frac{\partial\psi_0}{\partial\bar{z}} = 0,\ \theta_0 &= 0, C_0 = 0 \quad at \quad \eta = +1\end{aligned}\right\} \tag{12}$$

and to the first order are

$$\frac{\partial^2\theta_1}{\partial\eta^2} - (\alpha_1 f^2)\theta_1 = P_1 Rf\left(\frac{\partial\psi_0}{\partial\eta}\frac{\partial\theta_0}{\partial\bar{z}} - \frac{\partial\psi_0}{\partial\bar{z}}\frac{\partial\theta_0}{\partial\eta}\right) \tag{13}$$

$$\frac{\partial^2 C_1}{\partial\eta^2} = ScRf\left(\frac{\partial\psi_0}{\partial\eta}\frac{\partial C_0}{\partial\bar{z}} - \frac{\partial\psi_0}{\partial\bar{z}}\frac{\partial C_0}{\partial\eta}\right) \tag{14}$$

$$\frac{\partial^4\psi_1}{\partial\eta^4} - (M_1^2 f^2)\frac{\partial^2\psi_1}{\partial\eta^2} = -\frac{Gf^3}{R}\left(\frac{\partial\theta_1}{\partial\eta} + N\frac{\partial C_1}{\partial\eta}\right) + Rf\left(\frac{\partial\psi_0}{\partial\eta}\frac{\partial^3\psi_0}{\partial z^3} - \frac{\partial\psi_0}{\partial\bar{z}}\frac{\partial^3\psi_0}{\partial x\partial z^2}\right) \tag{15}$$

with

$$\left.\begin{array}{c} \psi_1(+1) - \psi_1(-1) = 0 \\ \frac{\partial\psi_1}{\partial\eta} = 0, \frac{\partial\psi_1}{\partial\bar{z}} = 0,\ \theta_1 = 0, C_1 = 0 \quad at \quad \eta = -1 \\ \frac{\partial\psi_1}{\partial\eta} = 0, \frac{\partial\psi_1}{\partial\bar{z}} = 0,\ \theta_1 = 0, C_1 = 0 \quad at \quad \eta = +1 \end{array}\right\} \tag{16}$$

Solving the Eq. (9)-(10) subject to the boundary conditions in Eq. (11). We obtain

$$\theta_{0_0} = 0.5\left(\frac{Ch(h\eta)}{Ch(h)} - \frac{Sh(h\eta)}{Sh(h)}\right)$$

$$C_0 = 0.5(1-\eta)$$

$$\psi_0 = a_{11}Cosh(\beta_1\eta) + a_{12}Sinh(\beta_1\eta) + a_{15}\eta + a_{14} + \phi_1(\eta)$$

$$\phi_1(\eta) = a_8\eta^2 - a_9 Sh(h\eta) - a_{10}Ch(h\eta) + 2a_8\eta - a_9 hCh(h\eta) - a_{10}hSh(h\eta)$$

Similarly, the solutions to the first order are

$$\theta_1 = a_{34}Ch(h\eta) + a_{35}Sh(h\eta) + \phi_2(\eta)$$

$$\phi_2(\eta) = a_{14} + a_{15}\eta + (a_{16} + a_{18}\eta + a_{25}\eta^2)Ch(h\eta) + (a_{17} + a_{19}\eta + +a_{24}\eta^2)Sh(h\eta) + (a_{20} + a_{22}\eta)Ch(2h\eta) + (a_{21} + a_{23}\eta)Sh(2h\eta) + a_{26}\eta Sh(\beta_2\eta) + a_{27}\eta Sh(\beta_3\eta) + a_{28}\eta Ch(\beta_2\eta) + a_{29}\eta Ch(\beta_3\eta) + a_{30}Ch(\beta_2\eta) + (a_{21} + a_{23}\eta)Sh(2h\eta) + a_{26}\eta Sh(\beta_2\eta) + a_{27}\eta Sh(\beta_3\eta) + a_{28}\eta Ch(\beta_2\eta) + a_{29}\eta Ch(\beta_3\eta) + a_{30}Ch(\beta_2\eta)$$

$$C_1 = a_{36}(\eta^2 - 1) + a_{37}(\eta^3 Sh(\beta_1\eta) - Sh(\beta_1)) + a_{38}\eta(Ch(\beta_1\eta) - Ch(\beta_1)) + (a_{39} + a_{53})(\eta Sh(\beta_1\eta) - Sh(\beta_1)) + (a_{40} + a_{52} + a_{50})\eta(Ch(\beta_1\eta) - Ch(\beta_1)) + (a_{41} + a_{60} + \eta(a_{64} - a_{47}))\eta(Ch(\beta_1\eta) - Ch(\beta_1)) + +(a_{40} + a_{52} + a_{50})\eta(Ch(\beta_1\eta) - Ch(\beta_1)) + (a_{41} + a_{60} + \eta(a_{64} - a_{47}))\eta(Ch(\beta_1\eta) - Ch(\beta_1)) + (a_{62} - a_{41} + \eta(a_{66} + a_{47}))xx(Ch(\beta_3\eta) - Ch(\beta_3)) + (a_{49} + a_{61})(Sh(\beta_2\eta) - \eta Sh(\beta_2 + (a_{63} + a_{49})(Sh(\beta_3\eta) - \eta Sh(\beta_3)) + (a_{42} + a_{56} + \eta(a_{45} + a_{58}))(Ch(2h\eta) - Ch(2h)) + (a_{57} + \eta a_{59})(Sh(2h\eta) - \eta Sh(2h)) + a_{51}(Sh(h\eta) - \eta Sh(h)) + a_{54}(\eta^2 Ch(h\eta) - Ch(h)) + a_{55}\eta(\eta sh(h\eta) - Sh(h)) + (a_{65} + a_{46})(\eta Sh(\beta_2\eta) - Sh(\beta_2)) + (a_{67} + a_{40})((\eta Sh(\beta_3\eta) - Sh(\beta_3)) + a_{48}((\eta Sh(2\beta_1\eta) - Sh(2\beta_1))$$

$$\psi_1 = b_{49}Cosh(\beta_1\eta) + b_{50}Sinh(\beta_1\eta) + b_{51}\eta + b_{52} + \phi_2(\eta)$$

$$\phi_2(\eta) = b_{21} + b_{22}\eta + b_{23}\eta^2 + b_{24}\eta^3 + b_{25}\eta^4 + b_{26}\eta^5 + b_{27}\eta^6 + b_{28}\eta^7 + (b_{29} + b_{30}\eta + b_{31}\eta^2 + b_{32}\eta^3 + b_{33}\eta^4 + b_{34}\eta^5 + b_{35}\eta^6)Cosh(\beta_1\eta) + (b_{36} + b_{37}\eta + b_{38}\eta^2 + b_{39}\eta^3 + b_{40}\eta^4 + b_{41}\eta^5 + b_{42}\eta^6)Sinh(\beta_1\eta) + b_{43}Cosh(2\beta_1\eta) + b_{44}Sinh(2\beta_1\eta)$$

where a_1, a_2, ……, a_{90}, and b_1, b_2, ……, b_{51} are constants.

4. Nusselt Number and Sherwood Number

The rate of heat transfer (Nusselt Number) on the walls has been calculated using the formula

$$Nu = \frac{1}{f(\theta_m - \theta_w)}\left(\frac{\partial\theta}{\partial\eta}\right)_{\eta=\pm1}$$

where

$$\theta_m = 0.5\int_{-1}^{1}\theta d\eta$$

$$(Nu)_{\eta=+1} = \frac{1}{f\theta_m}(a_{78} + \delta(a_{76} + a_{77}))$$

$$(Nu)_{\eta=-1} = \frac{1}{f(\theta_m - 1)}(a_{79} + \delta(a_{77} - a_{76})))$$

$$\theta_m = a_{80} + \delta a_{81}$$

The rate of mass transfer (Sherwood Number) on the walls has been calculated using the formula

$$Sh = \frac{1}{f(C_m - C_w)}\left(\frac{\partial C}{\partial\eta}\right)_{\eta=\pm1}$$

where

$$C_m = 0.5\int_{-1}^{1} C d\eta$$

$$(Sh)_{\eta=+1} = \frac{1}{fC_m}(a_{74} + \delta a_{70})$$

$$(Sh)_{\eta=-1} = \frac{1}{f(C_m - 1)}(a_{75} + \delta a_{71})$$

$$C_m = a_{73} + \delta a_{72}$$

5. Results and Discussion of the Numerical Methods

The results of figures and tables are explained in detail by considering particular figures and tables. Instead of ψ and ϕ I considered u and v to explain results and graphs |u| reduces with M≤4. Also, it enhances with Hall parameter (m) and Heat source parameter (α) Figure 2. higher the constriction of the channel walls larger |u| in the flow region Figure 3. When the molecular Buoyancy force dominates over the thermal buoyancy force, the secondary velocity enhances in magnitude

irrespective of the directions of the buoyancy forces Figure 4. lesser the molecular diffusivity larger |u| in the flow region Figure 5. An increase in the inclination of the magnetic field $\lambda \leq 0.5$, |u| depreciates and for higher $\lambda = 0.75$, it enhances and for still higher value of $\lambda = 1$ it decreases in magnitude. Higher the Lorentz force larger the actual temperature and for further higher Lorentz force lesser the actual temperature. The axial velocity enhances in the left region and reduces in the right region when the buoyancy forces act in the same direction and for the forces acting in opposite direction, the velocity decreases in left region and enhances in the right region Figure 6.

Figure 7 Represents the variation of v with M, m and α. It is found that higher the Lorentz force lesser the axial velocity in the flow region. An increase in the Hall parameter (m) enhances the axial velocity. Figure 8 and 9 depicts increase in the strength of the heat generating source (α) leads to a depreciation in the axial velocity. It is found that higher the constriction of the channel walls larger |v| in the flow region. When the molecular buoyancy force dominates over the thermal buoyancy force. The axial velocity enhances in the left region and reduces in the right region when the buoyancy forces act in the same direction and for the forces acting in opposite direction, the velocity decreases in left region and enhances in the right region Figure 10. The variation of v Schmidt number (Sc) shows that lesser the molecular diffusivity smaller v in the flow region Figure 11.

Figure 12 represents the temperature enhances with increase in the Hall parameter $m \leq 1.5$ and reduces with higher values of $m \geq 2.5$. An increase in the heat source parameter α leads to decreases in the temperature. Figure 13 shows the variation of beta increasing beta decreases the levels of temperature. Whereas Figure 14 represent the increase in variation of N decreases with temperature and Figure 15 shows the variation of Schmidt number increase in Schmidt number shows the increase in temperature level. Higher the constriction of the channel walls lesser the temperature except in narrow region adjacent to $\eta = 1$ and for further higher constriction larger the actual temperature and for still higher constriction lesser the temperature except in the region $0.4 \leq \eta \leq 0.8$. The temperature reduces when the buoyancy forces act in the same direction and for the forces acting in opposite directions the temperature enhances in the entire flow region. Lesser the molecular diffusivity larger the temperature in the left half and lesser in the right half and for further lowering of the molecular diffusivity lesser the temperature in the let half and larger in the right half Figure 16. The temperature enhances with inclination $\lambda \leq 0.75$ and reduces with higher $\lambda = 1$.

The concentration reduces with $M \leq 4$ and for higher $M \geq 6$, the concentration enhances in the left half and reduces in the right half. Figure 17 and 18 represents an increase in the Hall parameter $m \leq 1.5$ results in a decrease in the concentration and for higher $m \geq 2.5$ we notice an enhancement in the actual concentration. An increase in $\alpha \leq 4$ decreases the concentration and for higher $\alpha \geq 6$ it decreases except in the vicinity of $\eta = -1$. Higher the constriction of the channel walls larger the actual concentration and for higher constriction lesser the actual concentration and for still higher constriction of the channel walls lesser the concentration in the left half and larger in the right half Figure 19. the actual concentration enhances in the flow region except in the region $0.4 \leq \eta \leq 0.8$ where it decreases when the buoyancy forces act in the same direction and for the forces acting in opposite direction the actual concentration decreases in the left half and enhances in the right half Figure 20. Lesser the molecular diffusivity smaller the concentration in the flow field Figure 21.

In Table 1-16 at $\eta = +1$, the rate of heat transfer enhances with m for G>0 and decreases for G<0. At $\eta = -1$, |Nu| enhances with $m \leq 1.5$ and decreases s with higher $m \geq 2.5$. Higher the constriction of the channel walls larger |Nu| and for higher constriction ($|\beta| \geq 0.7$), we notice a decrease at $\eta = +1$ and at η=-1, larger |Nu| for G. The rate of heat transfer at $\eta = +1$ decreases with increase in $\lambda \leq 0.75$ and enhances with $\lambda \geq 1$, while at $\eta = -1$, |Nu| d decreases with $\lambda \leq 0.5$ and enhances with higher $\lambda \geq 0.75$. Higher the constriction of the channel walls lesser |Sh|. An increase in the inclination

λ of the magnetic field ($\lambda \leq 0.5$) and the rate of mass transfer enhances and decreases with higher $\lambda \geq 0.75$, at both the walls.

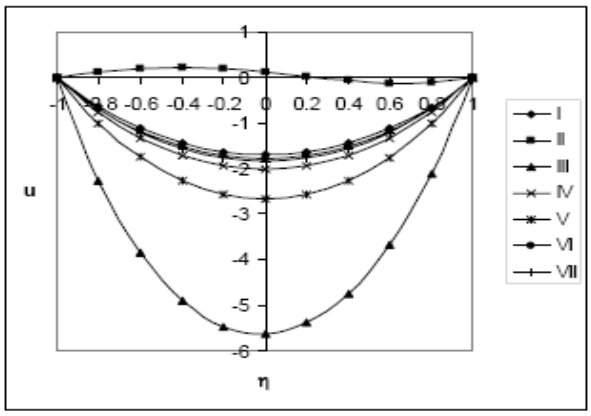

	I	II	III	IV	V	VI	VII
M	2	4	6	2	2	2	
m	0.5	0.5	0.5	1.5	2.5	0.5	0.5
α	2	2	2	2	2	4	6

Fig. 2. Variation of u with M, m, α

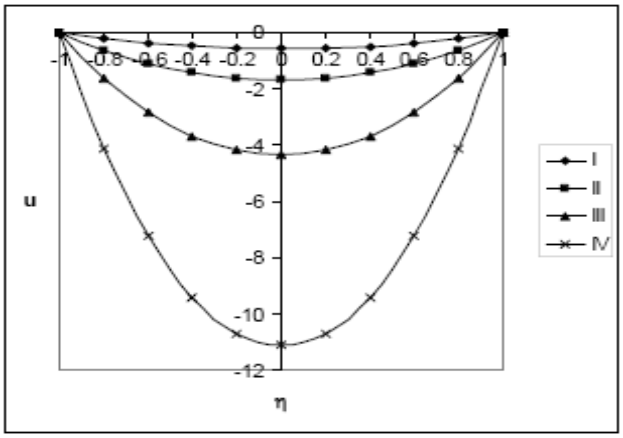

	I	II	III	IV
β	-0.3	-0.5	-0.7	-0.9

Fig. 3. Variation of u with β

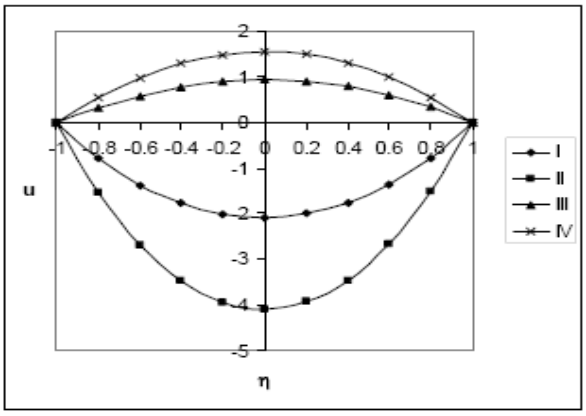

	I	II	III	IV
N	1	2	-0.5	-0.8

Fig. 4. Variation of u with N

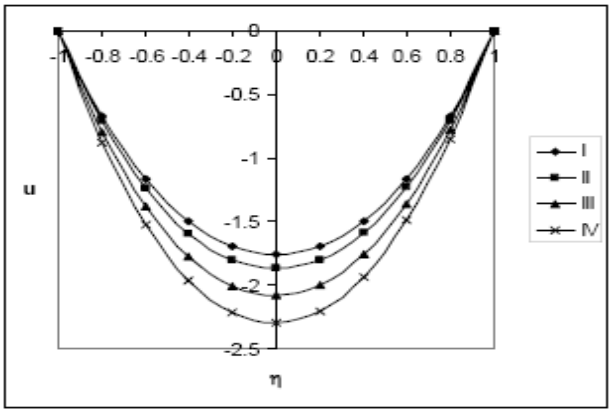

	I	II	III	IV
Sc	0.24	0.6	1.3	2.01

Fig. 5. Variation of u with Sc

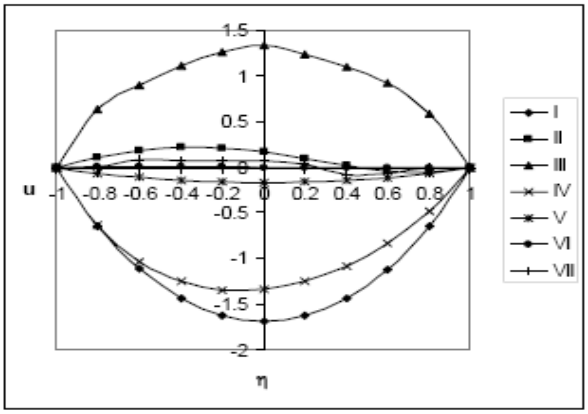

	I	II	III	IV	V	VI	VII
λ	0.25	0.5	0.75	1	0.5	0.5	0.5
x	π/4	π/4	π/4	π/4	π/2	π	2π

Fig. 6. Variation of u with λ, x

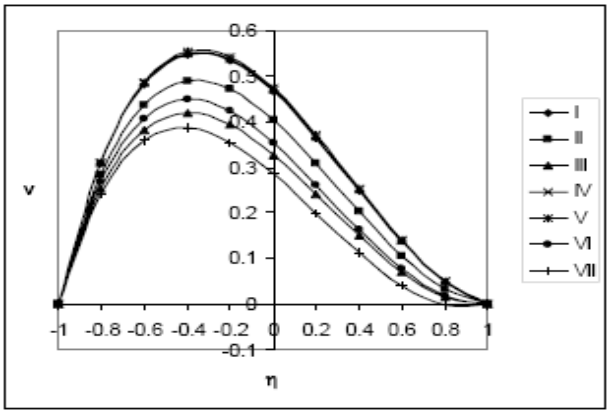

	I	II	III	IV	V	VI	VII
M	2	4	6	2	2	2	2
m	0.5	0.5	0.5	1.5	2.5	0.5	0.5
α	2	2	2	2	2	4	6

Fig. 7. Variation of v with M, m, α

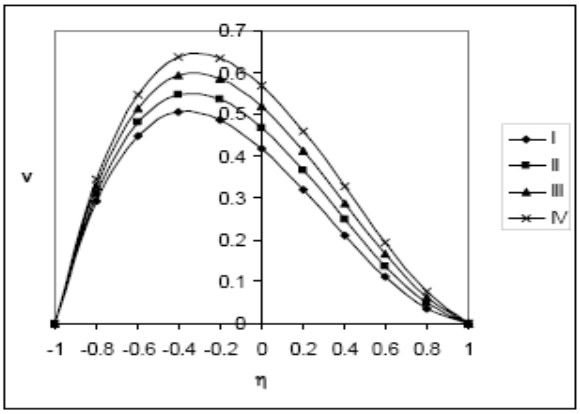

	I	II	III	IV
β	-0.3	-0.5	-0.7	-0.9

Fig. 8. Variation of v with β

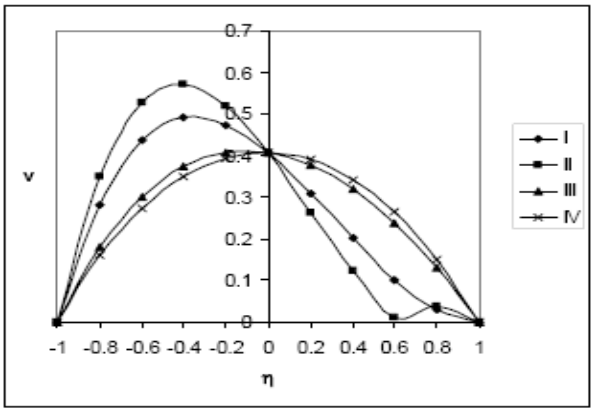

	I	II	III	IV
N	1	2	-0.5	-0.8

Fig. 9. Variation of v with N

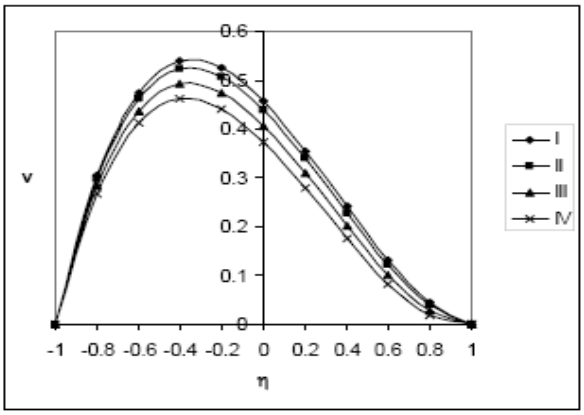

	I	II	III	IV
Sc	0.24	0.6	1.3	2.01

Fig. 10. Variation of v with Sc

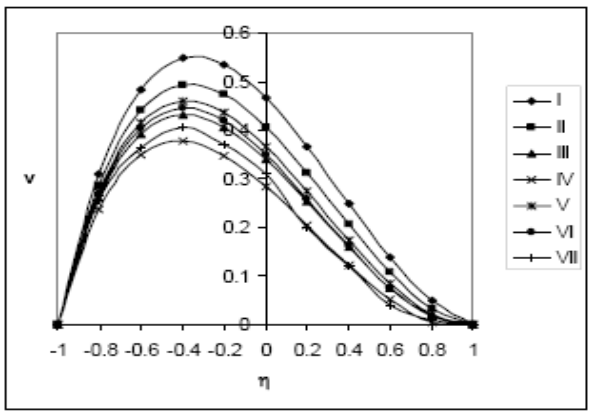

	I	II	III	IV	V	VI	VII
λ	0.25	0.5	0.75	1	0.5	0.5	0.5
x	π/4	π/4	π/4	π/4	π/2	π	2π

Fig. 11. Variation of v with λ, x

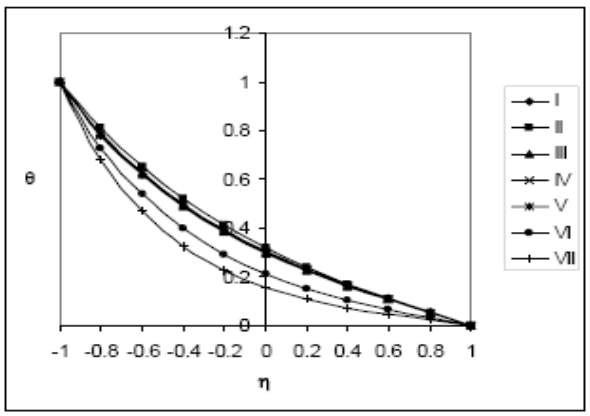

	I	II	III	IV	V	VI	VII
M	2	4	6	2	2	2	2
m	0.5	0.5	0.5	1.5	2.5	0.5	0.5
α	2	2	2	2	2	4	6

Fig. 12. Variation of θ with M, m, α

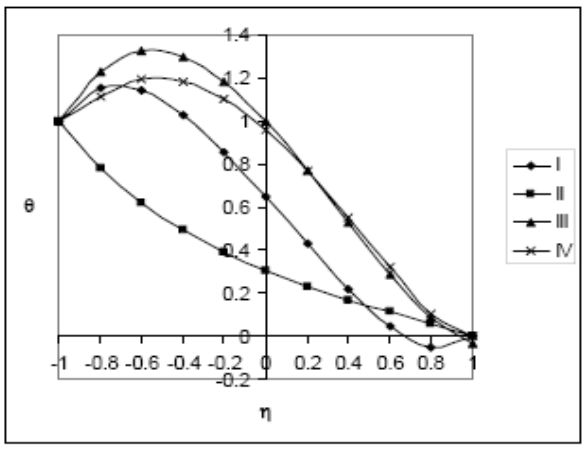

	I	II	III	IV
β	-0.3	-0.5	-0.7	-0.9

Fig. 13. Variation of θ with β

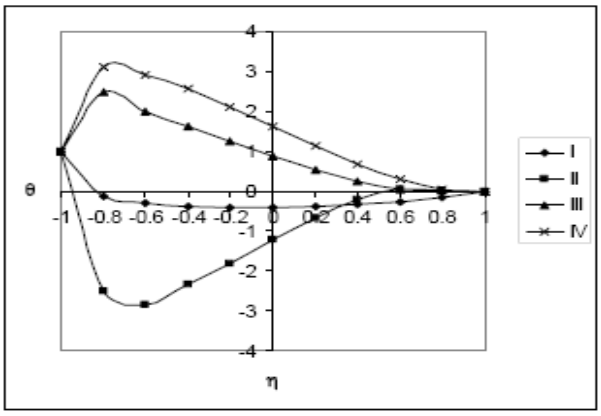

	I	II	III	IV
N	1	2	-0.5	-0.8

Fig. 14. Variation of θ with N

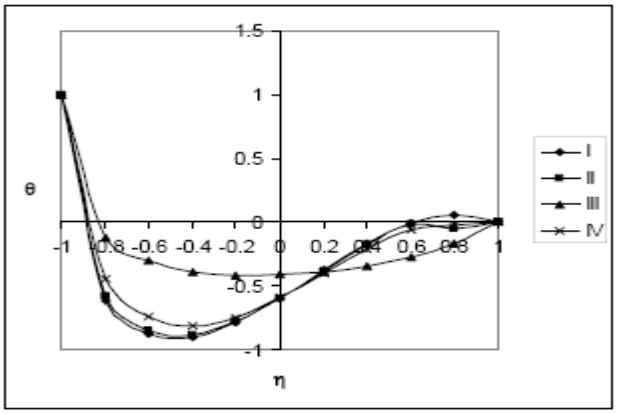

	I	II	III	IV
Sc	0.24	0.6	1.3	2.01

Fig. 15. Variation of θ with Sc

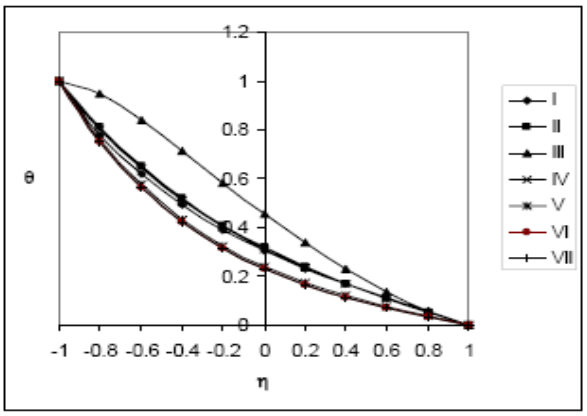

	I	II	III	IV	V	VI	VII
λ	0.25	0.5	0.75	1	0.5	0.5	0.5
x	π/4	π/4	π/4	π/4	π/2	π	2π

Fig. 16. Variation of θ with λ, x

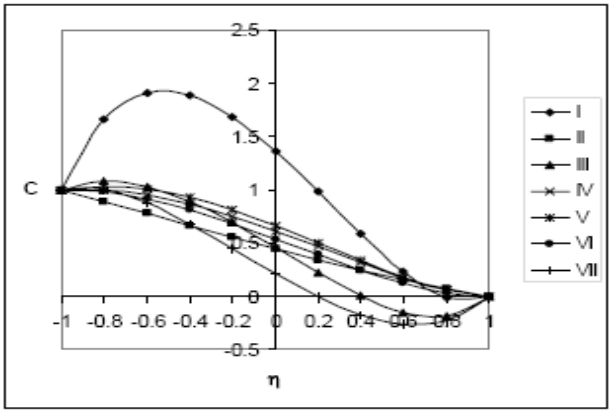

	I	II	III	IV	V	VI	VII
M	2	4	6	2	2	2	2
m	0.5	0.5	0.5	1.5	2.5	0.5	0.5
α	2	2	2	2	2	4	6

Fig. 17. Variation of C with M, m, α

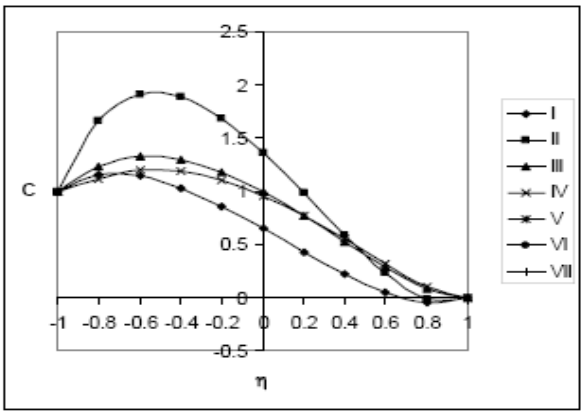

	I	II	III	IV
β	-0.3	-0.5	-0.7	-0.9

Fig. 18. Variation of C with β

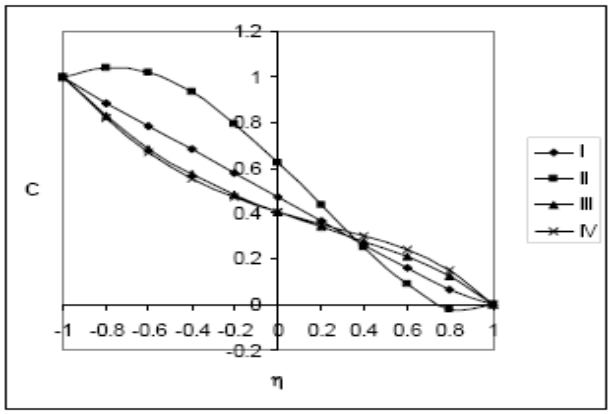

	I	II	III	IV
N	1	2	-0.5	-0.8

Fig. 19. Variation of C with N

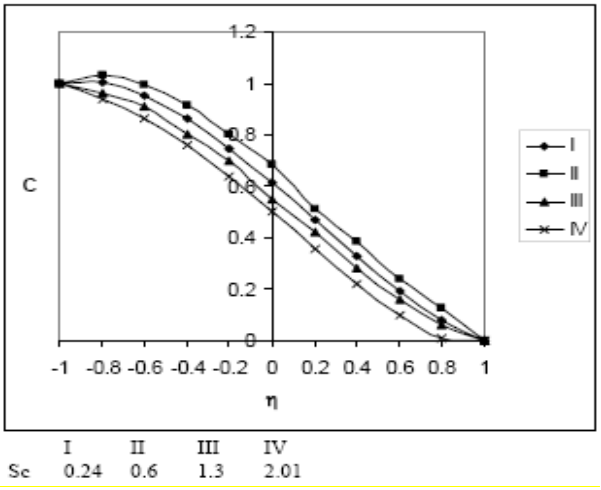

Fig. 20. Variation of C with Sc

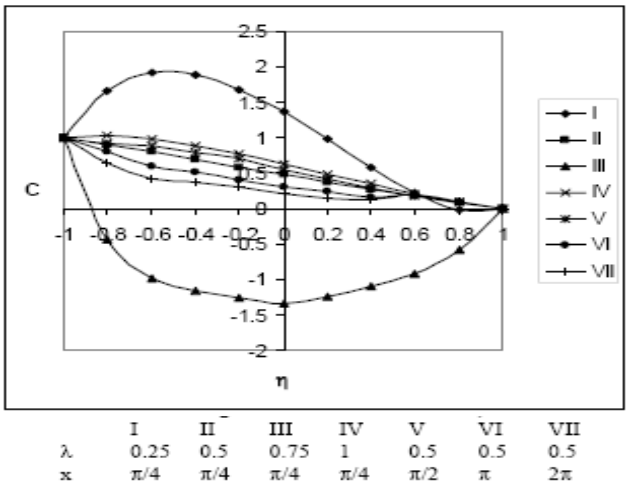

Fig. 21. Variation of C with λ, x

Table 1
Nusselt Number (Nu) at $\eta = 1$

G	I	II	III	IV	V	VI	VII
10^3	-11.98829	-42.793	-0.50763	-1.88259	-2.05014	-2.44022	-21.17508
$3X10^3$	-2.14927	8.02139	-0.4443	-2.23234	-2.3966	-13.00948	-99.75994
-10^3	-17.1206	-0.27554	-0.3272	-13.55019	-7.73351	8.84851	9.47034
$-3X10^3$	-4.72538	0.51007	-0.35795	-4.4215	-4.14614	22.58604	15.3519
M	2	4	6	2	2	2	2
m	0.5	0.5	0.5	1.5	2.5	0.5	0.5
α	2	2	2	2	2	4	6

Table 2
Nusselt Number (Nu) at $\eta = 1$

G	I	II	III	IV	V	VI
10^3	-6.3484	-11.98829	-4.22639	-1.80165	-5.78081	-2.21439
$3X10^3$	-2.61933	-2.84927	-1.40821	-0.73513	-2.2412	-2.13254
-10^3	1.76734	-17.1206	-1.95859	-0.6937	-20.51178	-9.31945
$-3X10^3$	9.59863	-10.72538	-1.6939	-0.70968	-4.39197	-3.79054
β	-0.3	-0.5	-0.7	-0.9	-0.5	-0.5
R	35	35	35	35	70	140

Table 3
Nusselt Number (Nu) at $\eta = 1$

G	I	II	III	IV	V	VI	VII
10^3	-11.9882	0.5053	0.4699	0.9917	-0.9949	-0.9456	-0.9982
$3X10^3$	-2.1493	0.8067	0.6015	7.1883	-2.5462	-1.1459	-1.1649
-10^3	-17.1206	-0.1996	0.06167	-0.6341	0.3756	-0.2681	-0.6188
$-3X10^3$	-4.7254	0.6361	0.06114	-0.8956	1.7449	-0.3662	-0.3677
λ	0.25	0.5	0.75	1.	0.25	0.25	0.25
x	$\pi/4$	$\pi/4$	$\pi/4$	$\pi/4$	$\pi/2$	π	2π

Table 4
Nusselt Number (Nu) at $\eta = 1$

G	I	II	III	IV	V	VI	VII
10^3	-1.2224	-1.1746	-1.7313	-1.7012	-1.6972	4.7913	-9.7376
$3X10^3$	-1.6751	-1.4406	-2.0569	-1.9226	-1.8645	-4.5539	-5.1542
-10^3	-1.3531	-5.9749	-6.9413	1.5329	-3.0464	-1.3324	-1.4712
$-3X10^3$	-0.4321	-2.4587	-4.3874	0.6015	-2.4531	-1.5762	-1.6995
Sc	1.3	2.01	0.24	0.6	1.3	1.3	1.3
N	1	1	1	1	2	-0.5	-0.8

Table 5
Nusselt Number (Nu) at $\eta = -1$

G	I	II	III	IV	V	VI	VII
10^3	-5.0163	-0.928646	3.530498	-9.47244	-7.895881	19.16804	10.36107
$3X10^3$	-7.529252	-1.649825	3.300662	-7.038785	-6.234847	56.98809	22.9403
-10^3	-3.187133	-7.560344	2.723109	-3.272533	-3.290047	-11.43055	-21.4962
$-3X10^3$	-4.18854	-4.399603	2.899336	-4.12201	-4.048025	-21.49378	-83.29836
M	2	4	6	2	2	2	2
m	0.5	0.5	0.5	1.5	2.5	0.5	0.5
α	2	2	2	2	2	4	6

Table 6
Nusselt Number (Nu) at $\eta = -1$

G	I	II	III	IV	V	VI
10^3	19.05358	-5.0163	-4.228974	-2.21112	-64.65746	-13.07395
$3X10^3$	-69.06149	-7.529252	-3.269913	-1.356228	-7.719963	-8.129309
-10^3	-2.398982	-3.187133	-2.219865	-1.027081	-3.089025	-2.908075
$-3X10^3$	-4.5444	-2.18854	-2.539345	-1.134496	-4.115279	-3.975556
β	-0.3	-0.5	-0.7	-0.9	-0.5	-0.5
R	35	35	35	35	70	140

Table 7
Nusselt Number (Nu) at $\eta = -1$

G	I	II	III	IV	V	VI	VII
10^3	-16.1298	-1.1345	-0.4504	13.8105	3.8443	1.4082	1.3931
$3X10^3$	-7.5292	-0.0281	-0.4695	13.4541	7.3836	1.2263	1.2197
-10^3	-3.1872	-1.5282	-0.4868	12.1384	-0.3369	1.6519	1.6528
$-3X10^3$	-4.1885	-2.0777	0.4757	12.6205	-2.0477	1.7508	1.7526
λ	0.25	0.5	0.75	1.	0.25	0.25	0.25
x	$\pi/4$	$\pi/4$	$\pi/4$	$\pi/4$	$\pi/2$	π	2π

Table 8
Nusselt Number (Nu) at $\eta = -1$

G	I	II	III	IV	V	VI	VII
10^3	1.4803	-8.4233	-10.3159	-8.9816	-6.5373	-2.2998	-2.9753
$3X10^3$	-6.6358	-7.2255	-7.3483	-7.0912	-5.7028	-3.3995	-3.8068
-10^3	-1.8095	-3.6264	-4.1138	-2.5523	-4.3964	-7.7243	-6.6504
$-3X10^3$	-2.1215	-4.6424	-5.1298	-3.2595	-5.1295	-8.1249	-7.2509
Sc	1.3	2.01	0.24	0.6	1.3	1.3	1.3
N	1	1	1	1	2	-0.5	-0.8

Table 9
Sherwood number (Sh) at $\eta = 1$

G	I	II	III	IV	V	VI	VII
10^3	-1.04422	-14.17238	-20.50905	-0.23277	-0.12739	-0.36263	-1.23054
$3X10^3$	-1.67511	-26.67278	-20.5356	-1.16585	-0.63459	-1.28821	-2.80625
-10^3	0.1291	-14.26308	-15.80429	0.09063	0.04856	0.08326	0.93316
$-3X10^3$	1.14436	-24.01008	-18.07686	0.82719	0.47362	1.09847	3.19485
M	2	4	6	2	2	2	2
m	0.5	0.5	0.5	1.5	2.5	0.5	0.5
α	2	2	2	2	2	4	6

Table 10
Sherwood number (Sh) at $\eta = 1$

G	I	II	III	IV	V	VI
10^3	-22.64324	-1.04422	-0.08541	-0.01474	-0.15159	-0.47703
$3X10^3$	-10.35031	-1.67511	-0.41006	-0.09851	-0.50364	-0.16276
-10^3	0.38005	0.1291	0..02957	0.00042	-0.00423	-0.03286
$-3X10^3$	3.51584	1.14436	0.34735	0.08644	0.21816	-0.30646
β	-0.3	-0.5	-0.7	-0.9	-0.5	-0.5
R	35	35	35	35	70	140

Table 11
Sherwood number (Sh) at $\eta = 1$

G	I	II	III	IV	V	VI	VII
10^3	-1.0447	34.8689	-3.6787	2.6987	1.9024	2.2523	1.2614
$3X10^3$	-1.6788	-21.8316	-5.5578	3.9904	1.2959	18.9527	18.9414
-10^3	0.1287	-20.7239	-3.8064	0.9058	0.8438	0.9309	0.9301
$-3X10^3$	1.1448	-30.2709	-5.6257	3.0247	10.1019	17.8433	17.8379
λ	0.25	0.5	0.75	1.	0.25	0.25	0.25
x	$\pi/4$	$\pi/4$	$\pi/4$	$\pi/4$	$\pi/2$	π	2π

Table 12
Sherwood number (Sh) at $\eta = 1$

G	I	II	III	IV	V	VI	VII
10^3	-0.2482	-0.2364	-1.9853	-1.0816	-0.2234	0.2125	0.0903
$3X10^3$	-1.6703	-1.0749	-3.1652	-3.9247	-0.9535	3.0791	1.7714
-10^3	0.1406	0.0908	0.8059	0.3181	0.0861	-0.5733	-0.2436
$-3X10^3$	1.1518	0.7803	5.2142	2.0245	0.6505	-3.2814	-1.7468
Sc	1.3	2.01	0.24	0.6	1.3	1.3	1.3
N	1	1	1	1	2	-0.5	-0.8

Table 13
Sherwood number (Sh) at $\eta = - 1$

G	I	II	III	IV	V	VI	VII
10^3	-2.294783	4.774063	9.085408	-0.08165	-0.031178	-0.115872	-0.431864
$3X10^3$	3.078805	18.98452	9.809118	0.711211	0.342909	-0.378887	-0.499336
-10^3	0.068704	-3.966851	7.669532	0.068309	0.061456	0.33736	0.375243
$-3X10^3$	-0.712843	11.85803	9.052016	-0.482359	-0.23703	0.818546	0.91194
M	2	4	6	2	2	2	2
m	0.5	0.5	0.5	1.5	2.5	0.5	0.5
α	2	2	2	2	2	4	6

Table 14
Sherwood number (Sh) at η = - 1

G	I	II	III	IV	V	VI
10^3	-14.24577	-2.294783	-0.143922	-0.021857-	-0.638146	-0.602033
$3X10^3$	7.6109111	1.078805	0.248394	0.059321	0.159005	-0.08895
-10^3	0.0188	0.008704	0.041318	0.018524	0.086838	0.063949
$-3X10^3$	-2.565435	-0.712843	-0.198233	-0.046828	-0.022447	0.08898
β	-0.3	-0.5	-0.7	-0.9	-0.5	-0.5
R	35	35	35	35	70	140

Table 15
Sherwood number (Sh) at η = - 1

G	I	II	III	IV	V	VI	VII
10^3	-2.2947	15.1985	1.9234	-0.7189	-1.4391	-1.1559	-1.2615
$3X10^3$	1.0788	22.4488	3.7801	-2.6257	-0.546894	-19.1098	-19.0966
-10^3	0.0687	-12.6629	1.9597	-0.3551	-0.3205	-0.9236	-0.9041
$-3X10^3$	-0.7128	19.1734	3.8023	-2.3054	0.15062	-17.9767	-17.9691
λ	0.25	0.5	0.75	1.	0.25	0.25	0.25
x	$\pi/4$	$\pi/4$	$\pi/4$	$\pi/4$	$\pi/2$	π	2π

Table 16
Sherwood number (Sh) at η = - 1

G	I	II	III	IV	V	VI	VII
10^3	0.02482	0.0189	-0.1728	-0.0598	-0.0132	-0.4494	-0.3328
$3X10^3$	1.1296	0.7499	8.4591	2.5755	0.4063	-3.6973	-2.3608
-10^3	0.0302	0.0056	0.1419	-0.1321	0.1142	1.1626	0.6344
$-3X10^3$	-0.7854	-0.5004	-3.3683	-1.6736	-0.2439	3.9973	2.3435
Sc	1.3	2.01	0.24	0.6	1.3	1.3	1.3
N	1	1	1	1	2	-0.5	-0.8

6. Conclusions

In the present paper we investigate the convective study heat and mass transfer flow of a viscous electrically conducting fluid in a vertical wavy channel under the influence of an inclined magnetic fluid with heat generating sources. The walls of the channels are maintained at constant temperature and concentration. The equations governing the flow heat and concentration are solved by employing perturbation technique with a slope δ of the wavy wall. The velocity, temperature and concentration distributions are investigated for a different value of G, M, m, Sc, N, N_1, α and x. The rate of heat and mass transfer are numerically evaluated for a different variation of the governing parameters. Few important results noted below

i. An increase in the Hall parameter (m) enhances the axial velocity. An increase in the strength of the heat generating source (α) leads to a depreciation in the axial velocity.
ii. It is found that higher the constriction of the channel walls larger |v| in the flow region.
iii. When the molecular Buoyancy force dominates over the thermal Buoyancy force. The axial velocity enhances in the left region and reduces in the right region when the Buoyancy forces act in the same direction and for the forces acting in opposite direction, the velocity depreciates in left region and enhances in the right region.
iv. When the molecular Buoyancy force dominates over the thermal Buoyancy force, the secondary velocity enhances in magnitude irrespective of the directions of the Buoyancy forces

v. The actual temperature reduces when the Buoyancy forces act in the same direction and for the forces acting in opposite directions the actual temperature enhances in the entire flow region.
vi. Lesser the molecular diffusivity larger the actual temperature in the left half and lesser in the right half and for further lowering of the molecular diffusivity lesser the actual temperature in the let half and larger in the right half.
vii. The actual temperature enhances with inclination $\lambda \leq 0.75$ and reduces with higher $\lambda = 1$.
viii. Higher the constriction of the channel walls larger the actual concentration and for higher constriction lesser the actual concentration and for still higher constriction of the channel walls lesser the concentration in the left half and larger in the right-side.

Acknowledgment
This research was not funded by any grant.

References

[1] Khaleque, Tania S., and M. A. Samad. "Effects of radiation, heat generation and viscous dissipation on MHD free convection flow along a stretching sheet." *Research Journal of Applied Sciences, Engineering and Technology* 2, no. 4 (2010): 368-377.
[2] Amkadni, Maryem, and Adnane Azzouzi. "On a similarity solution of MHD boundary layer flow over a moving vertical cylinder." *International Journal of Differential Equations* 2006 (2006). https://doi.org/10.1155/DENM/2006/52765
[3] Rajeswari, R., B. Jothiram, and V. K. Nelson. "Chemical reaction, heat and mass transfer on nonlinear MHD boundary layer flow through a vertical porous surface in the presence of suction." *Applied Mathematical Sciences* 3, no. 49-52 (2009): 2469-2480.
[4] England, W. G., and A. F. Emery. "Thermal radiation effects on the laminar free convection boundary layer of an absorbing gas." *Journal of Heat Transfer* 91, no. 1 (1969): 37-44. https://doi.org/10.1115/1.3580116
[5] Hossain, M. A., and H. S. Takhar. "Radiation effect on mixed convection along a vertical plate with uniform surface temperature." *Heat and Mass Transfer* 31, no. 4 (1996): 243-248. https://doi.org/10.1007/s002310050052
[6] Raptis, A., and C. Perdikis. "Radiation and free convection flow past a moving plate." *Applied Mechanics and Engineering* 4, no. 4 (1999): 817-821.
[7] Das, U. N., R. K. Deka, and V. M. Soundalgekar. "Radiation effects on flow past an impulsively started vertical infinite plate." *Journal of Theoretical and Applied Mechanics* 1 (1996): 111-115.
[8] Lavanya, B. "Unsteady MHD Convective laminar flow between two Vertical Porous plates with mass transfer." *Journal of Mechanical Engineering Research and Developments* 41, no. 1 (2018): 97-109.
[9] Nagasasikala, Madduleti, and Bommanna Lavanya. "Effects of Dissipation and Radiation on Heat Transfer Flow of a Convective Rotating Cuo-Water Nano-fluid in a Vertical Channel." *Journal of Advanced Research in Fluid Mechanics and Thermal Sciences* 50, no. 2 (2018): 108-117.
[10] Nagasasikala, Madduleti, and Bommanna Lavanya. "Heat and mass transfer of a MHD flow of a nanofluid through a porous medium in an annular, circular region with outer cylinder maintained at constant heat flux." *CFD Letters* 11, no. 9 (2019): 32-58.
[11] Ahmed, N., and D. Kalita. "Transient MHD free convection from an infinite vertical porous plate in a rotating system with mass transfer and Hall current." *Journal of Energy, Heat and Mass Transfer* 33, no. 3 (2011): 271-292.
[12] Hayat, T., S. B. Khan, M. Sajid, and S. Asghar. "Rotating flow of a third grade fluid in a porous space with Hall current." *Nonlinear Dynamics* 49, no. 1-2 (2007): 83-91. https://doi.org/10.1007/s11071-006-9105-1
[13] Narayana, PV Satya, G. Ramireddy, and S. Venkataramana. "Hall current effects on free convection MHD flow past a porous plate." *International Journal of Automotive and Mechanical Engineering* 3 (2011): 350-63. https://doi.org/10.15282/ijame.3.2011.10.0029
[14] Rani, Neela, and S. K. Tomar. "Thermal convection problem of micropolar fluid subjected to hall current." *Applied Mathematical Modelling* 34, no. 2 (2010): 508-519. https://doi.org/10.1016/j.apm.2009.06.007

[15] Bakr, A. A. "Effects of chemical reaction on MHD free convection and mass transfer flow of a micropolar fluid with oscillatory plate velocity and constant heat source in a rotating frame of reference." *Communications in Nonlinear Science and Numerical Simulation* 16, no. 2 (2011): 698-710. https://doi.org/10.1016/j.cnsns.2010.04.040

[16] Das, K. "Effect of chemical reaction and thermal radiation on heat and mass transfer flow of MHD micropolar fluid in a rotating frame of reference." *International Journal of Heat and Mass Transfer* 54, no. 15-16 (2011): 3505-3513. https://doi.org/10.1016/j.ijheatmasstransfer.2011.03.035

[17] Lavanya, Bommanna, and Madduleti Nagashasikala. "Effects of Chemical Reaction and Heat Generation on The Unsteady Free Convection Flow Past an Infinite Vertical Permeable Moving Plate with Variable Temperature." *Journal of Advanced Research in Fluid Mechanics and Thermal Sciences* 64, no. 2 (2019): 244-252.